Measurement of the depolarization parameter in elastic proton-proton scattering at 3 and 6 GeV/c*

G. W. Abshire,† G. W. Bryant, M. Corcoran, R. R. Crittenden, S. W. Gray, R. M. Heinz, A. W. Hendry, H. A. Neal,‡ and D. R. Rust
Department of Physics, Indiana University, Bloomington, Indiana 47401
(Received 16 June 1975)

Results are presented from an experiment designed to make the first systematic study of the depolarization parameter in elastic proton-proton scattering at high energies. Measurements were made at 3.0 and 6.0 GeV/c at $|t|$ values extending to 1.7 (GeV/c)^2 at the higher momentum. A high-intensity unpolarized proton beam was incident on a polarized proton target and the polarization of the elastically scattered recoil protons was determined with a carbon analyzer. The results are discussed in the framework of optical and exchange models.

We report herein the results of an experimental measurement of the Wolfenstein depolarization parameter[1] in elastic proton-proton scattering at 3.0 and 6.0 GeV/c. In the experiment a high-intensity unpolarized proton beam at the Argonne Zero Gradient Synchrotron (ZGS) was incident on a polarized proton target (PPT) and the polarization of the elastically scattered recoil protons was determined from the azimuthal double-scattering asymmetry exhibited in a carbon analyzer. Two multiwire proportional chamber spectrometers were used to detect and momentum-analyze the final-state protons to provide sufficient constraints to ensure elasticity. The measurements spanned the t region $0.3 < |t| < 1.7$ (GeV/c)^2.

The depolarization parameter (D) is an independent parameter of the proton-proton system. That is, its value cannot be inferred from the cross section and polarization or any of the other standard spin correlation parameters. It thus imposes additional constraints on the p-p scattering amplitudes. In the helicity formalism of Goldberger *et al.*[2] the depolarization is given by the relation

$$2\frac{d\sigma}{d\Omega}(1-D) = |\varphi_1 - \varphi_3|^2 + |\varphi_2 + \varphi_4|^2 , \tag{1}$$

where $d\sigma/d\Omega$ is the unpolarized differential cross section, and where the conventional set of helicity amplitudes are defined as follows:

$$\begin{aligned}
\varphi_1 &= \langle ++|\varphi|++\rangle , \\
\varphi_2 &= \langle ++|\varphi|--\rangle , \\
\varphi_3 &= \langle +-|\varphi|+-\rangle , \\
\varphi_4 &= \langle +-|\varphi|-+\rangle , \\
\varphi_5 &= \langle ++|\varphi|+-\rangle .
\end{aligned} \tag{2}$$

Note that φ_5, which is perhaps the dominant amplitude in determining the features of the polarization, does not explicitly appear in the above expression for the depolarization. In essentially all phenomenological analyses it is assumed that the double-helicity-flip amplitudes are negligible. To the extent that this assumption is valid, D is a direct measure of the difference in the two nonflip amplitudes φ_1 and φ_3. The structure of this difference is of substantial importance in testing various model predictions. It can be shown[3] that, in terms of experimentally observable quantities, D is given by

$$D = \frac{(1+PP_t)P_r - P}{P_t} , \tag{3}$$

where P_r is the polarization of the recoil protons resulting from the scattering of an unpolarized proton beam from a polarized target, P is the elastic p-p polarization parameter, and P_t is the target polarization along the normal to the scattering plane.

The experimental layout is shown in Fig. 1. A proton beam of intensity ~5×10^9/pulse was incident on a one-inch-long ~70% polarized proton target.[4] The final-state protons were detected and momentum-analyzed by the two multiwire proportional chamber spectrometers shown in the figure with a momentum resolution of ±6% and an effective opening angle resolution of 4 mrad. The relative time of flight of the two final-state protons was measured by counters $SC5$ and $FC5$ with a resolution of ±0.7 nsec. The trigger for the experiment required a coincidence between scintillation counters $FC1$, $FC3$, $FC5$, $SC1$, $SC3$, $SC4$, and $SC5$. Note that none of the trigger counters was downstream of the carbon analyzer. This feature eliminated one possible source of bias in the determination of the recoil proton polarization. Additional details of the spectrometer and the procedure used to select elastic events can be found in Ref. 5.

In Fig. 2 a typical momentum distribution of protons in the fast-proton spectrometer is shown be-

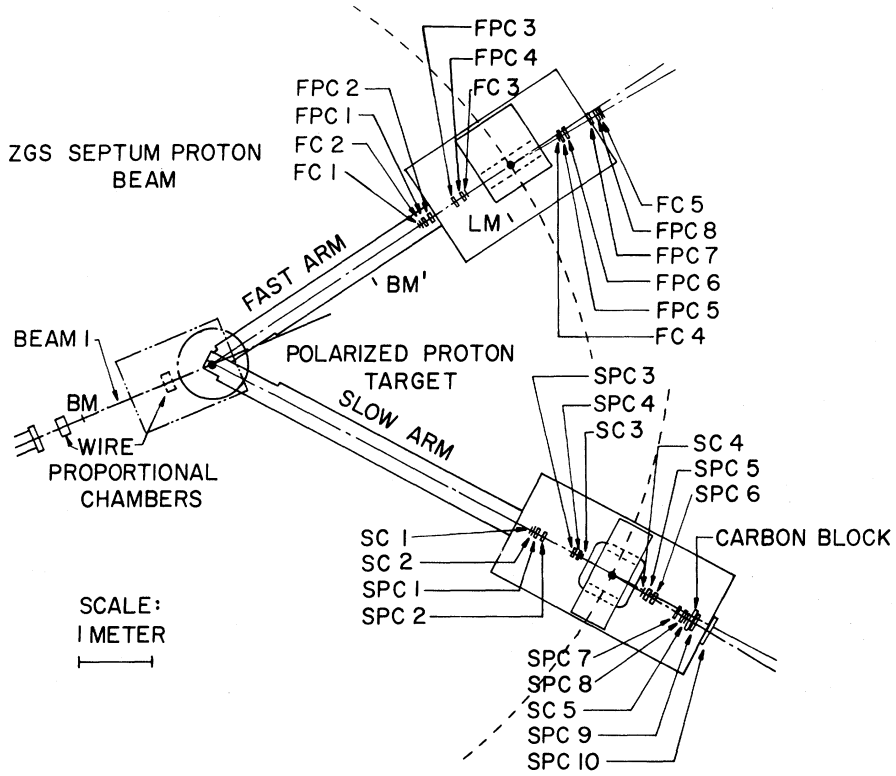

FIG. 1. The experimental layout. Elements labeled $SC1, \ldots, SC5$ and $FC1, \ldots, FC5$ are scintillation counters. Elements labeled $SPC1, \ldots, SPC10$ and $FPC1, \ldots, FPC8$ are multiwire proportional chambers. A magnet capable of bending elastically scattered protons through an angle $> 3°$ is present in each arm (between elements $SC3$ and $SC4$ and between elements $FC3$ and $FC4$). The angular position of each arm is remotely variable. BM, BM', and LM are beam monitors.

fore and after elastic cuts were applied to the slow-arm proton momentum distribution. As can be seen the remaining background is quite small. Results from dummy (carbon) target runs indicate that the peak which is observed in this figure is indeed predominantly due to scatters from free protons. A comparison of an uncut fast-proton momentum distribution for a corresponding set of dummy and propanediol target runs is shown in Fig. 3. When all elastic cuts have been applied, the remaining contamination from quasielastic and inelastic events is found to be less than ~12%. Furthermore, it has been determined from an analysis of the nonelastic data that the recoil proton polarization associated with this background makes a negligible contribution to the measured elastic depolarization.

The polarization of the recoil proton beam was measured by determining the left-right scattering asymmetry exhibited in its scattering from a carbon analyzer (of thickness $\frac{1}{2}$ in. to 2 in. depending on the t value being studied). Proportional chambers $SPC5$–$SPC8$ determined the recoil proton trajectory upstream of the carbon target, and cham-

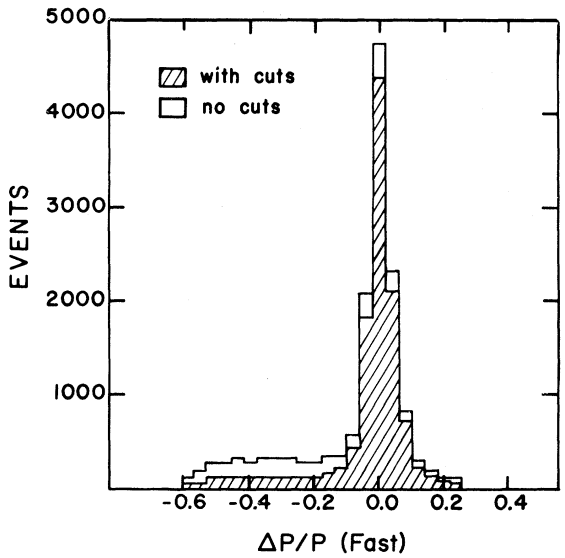

FIG. 2. Typical fast-proton momentum distribution at 6 GeV/c incident momentum and $\theta_{c.m.} = 30°$. The unshaded histogram corresponds to the uncut momentum distribution. The results of applying a ±20% cut on the slow-proton momentum are illustrated in the shaded histogram.

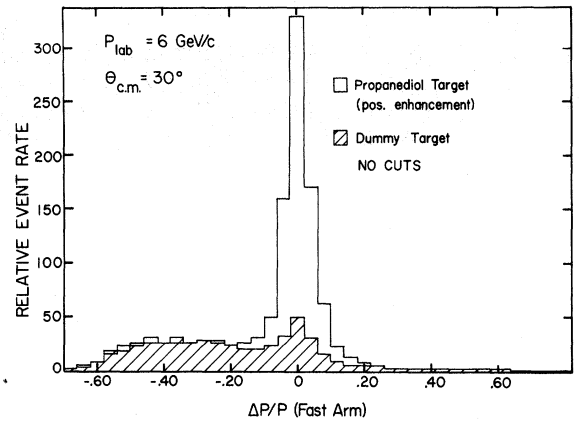

FIG. 3. The uncut fast-proton momentum distribution at 6 GeV/c, $\theta_{c.m.}$= 30° corresponding to normalized runs with a propanediol target and an equivalent dummy (carbon) target.

bers *SPC*9 and *SPC*10 determined the outgoing "double scattered" trajectory. Events with horizontally projected double scattering angles in the range $6° < \theta_c < 22°$ were utilized for the recoil proton polarization measurements. A typical double scattering vertex distribution along the nominal recoil proton trajectory is shown in Fig. 4. From this figure it is clear that the double scatters indeed originate in the carbon block.

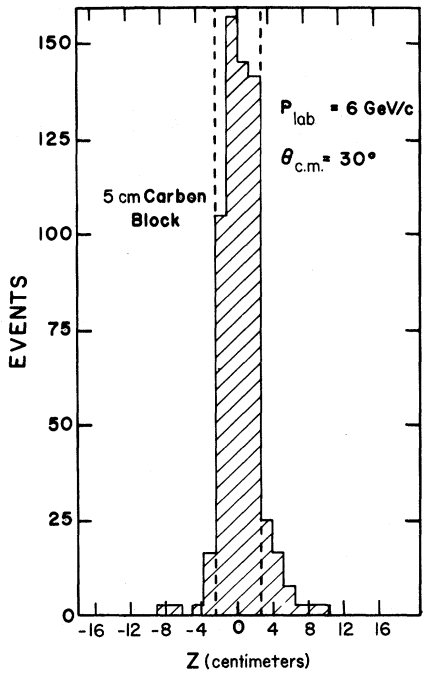

FIG. 4. Distribution of the reconstructed double scattering vertex along the nominal recoil proton beam trajectory for a typical run at 6 GeV/c, $\theta_{c.m.}$= 30°. The position of the 5-cm.-thick carbon analyzing block is indicated by the dashed lines.

The recoil proton polarization P_r is given by

$$P_r = \frac{\epsilon}{A}, \tag{4}$$

where ϵ is the left-right asymmetry $(L-R)/(L+R)$ and A is the effective carbon analyzing power corresponding to the proton energy and the geometry of the analyzer. In order to obtain precise values of the analyzing power a special auxiliary experiment was run with the polarimeter placed in the ZGS polarized proton beam. Knowledge of the beam polarization and the observed left-right double scattering asymmetry permitted a direct determination of the analyzing power. The systematic uncertainty in the analyzing power determined in this manner is roughly ±5% and is due primarily to the uncertainty in the polarization of the polarized beam. Three other independent approaches were employed to obtain checks on the values found for A. Since depolarization data were taken for both orientations of the target polarization the analyzer could be internally calibrated. However, because the effective beam polarization for such a calibration is just the elastic polarization P, which is small, the accuracy of this approach was very limited. We also used the extensive analyzing power measurements made by Surko[6] for polar scattering angles θ between 6° and 22°. From an analysis of our double scattering angle distributions it was possible to adapt the Surko measurements to the geometry of the present experiment. The modification of the Surko analyzing powers involved correcting for the difference in $\langle\cos\varphi\rangle_{av}$ in the two experiments (where φ is the azimuthal double scattering angle) and taking into account the effect of the large-θ scatters which are accepted within the projected angle limits of the present experiment. The systematic uncertainty associated with this procedure was estimated to be ±10%. Finally, we utilized p-C analyzing powers measured by Neal and Longo[7] for a polarimeter with a geometry similar to the one of the present experiment. A comparison of the various results is presented in Fig. 5. The smooth curve in this figure passes through the A values used in the calculation of D. It represents a fit to the A data obtained in the ZGS polarized beam calibration run at proton kinetic energies below 500 MeV. At kinetic energies above 500 MeV it is based on the Surko data and the condition that the analyzing power is virtually constant between 500 and 1000 MeV. Justification for this assumption comes from Ref. 7. It was not possible to directly calibrate the analyzer at the high-$|t|$ points because the bending power of the PPT magnet was not sufficient to bend

the polarized beam at these momenta into the recoil spectrometer at its minimum angle setting. However, the lack of direct calibration measurements at the high-$|t|$ points introduces an uncertainty in D which is estimated to be small compared with the statistical error.

Double scatters with an angle θ_c less than 6° are not very useful for polarization determination because of the small corresponding analyzing power. However, unless special provisions are made the bulk of the triggers will, of course, be associated with these small double scattering angles. One novel feature of the present experiment was a hardwired computer which sensed the status of the proportional chamber wires in the polarimeter and vetoed the recording of data corresponding to events with an unambiguous double scatter with $\theta_c < 3°$. In cases where multiple tracks were present in the chambers the computer allowed the event to be recorded in any case for later off-line filtering. Thus the hardware device produced no biases in the double scattering distribution but enhanced the number of useful double scatters in each data buffer by a factor of ~8. Figure 6 shows double scattering distributions with the polarimeter computer in operation. The asymmetry exhibited in Fig. 6(a) dramatically changed sign when the sense of the polarized target spin was flipped, as shown in Fig. 6(b).

A total of ~1 million triggers was recorded in the experiment. At a typical point approximately 50% of the triggers were due to elastic p-p interactions and 12% of the elastic events resulted in useful double scatters in the polarimeter. The trigger rate, with the polarimeter computer operational, varied from 2 to 46 per ZGS burst.

Several tests were made to ensure that no significant instrumental biases existed. "Straight-through" runs were frequently made with the polarimeter computer inactive to check that all elements of the polarimeter were properly aligned. Comparison of asymmetries from runs with and without the polarimeter computer verified that the device did not introduce an instrumental bias. Runs with the target unpolarized at $|t|$ values where the

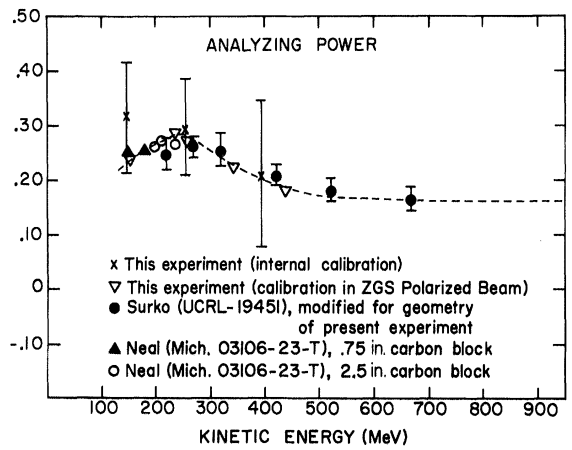

FIG. 5. p-C analyzing powers averaged over projected scattering angles in the interval $6° \leq \theta \leq 22°$. The crosses represent data from the internal calibration of the analyzer used in the present experiment. The open triangles represent data from an auxiliary calibration experiment utilizing the ZGS polarized beam. The solid circles represent data from Ref. 6, modified to correspond to the geometry of the present experiment. The open circles and the solid triangles represent data from Ref. 7, modified to correspond to the geometry of the present experiment. The dashed line represents the fit to the actual calibration data taken in the ZGS polarized beam (see text).

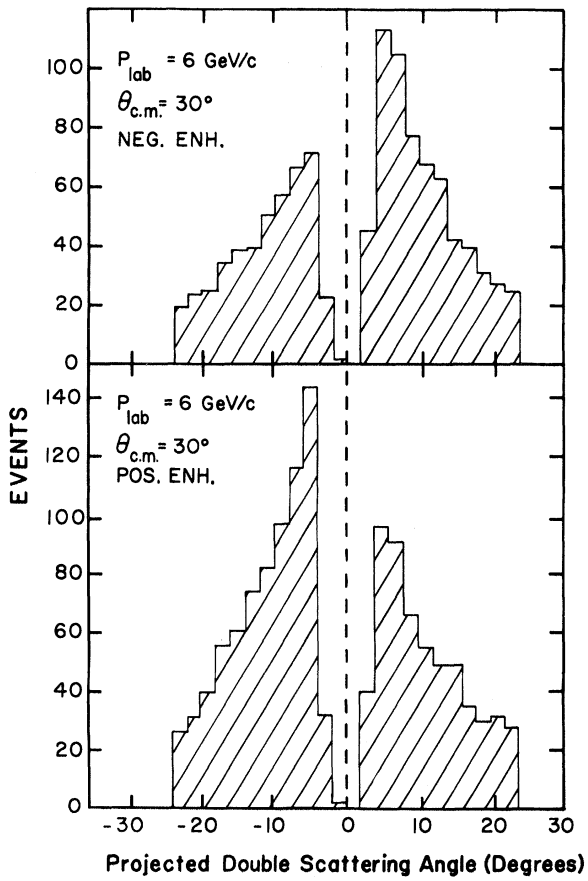

FIG. 6. Illustration of the effectiveness of the polarimeter computer in rejecting the recording of small-angle double scatters. Logic performed with outputs of the polarimeter proportional chambers vetoed the recording of events with unambiguous double scattering angles less than 3°. The left-right asymmetry seen in the upper histogram is almost completely reversed when the polarized target spin is reversed, as shown in the lower histogram.

TABLE I. Values of the depolarization parameter in proton-proton elastic scattering.

P_{lab} (GeV/c)	$\theta_{c.m.}$ (deg)	$-t$ [(GeV/c)^2]	D	ΔD
3.0	30	0.277	0.946	0.136
3.0	40	0.484	1.058	0.071
3.0	50	0.739	0.909	0.128
6.0	20	0.291	0.910	0.113
6.0	25	0.451	1.040	0.082
6.0	30	0.645	1.003	0.047
6.0	35	0.871	0.739	0.170
6.0	40	1.127	0.874	0.148
6.0	45	1.411	0.533	0.291
6.0	50	1.721	0.404	0.184

elastic polarization is small produced asymmetries consistent with zero. An analysis of the double scattering distributions from runs with a dummy target showed an insignificant asymmetry to be associated with the small quasielastic and inelastic background. The depolarization values determined from samples of data corresponding to different sections of the carbon target along the incident recoil beam was found to be consistent in all cases. This latter test was useful in verifying that we were indeed detecting reasonably elastic p-C scatters.

From Eq. (3) above it is clear that to determine D one requires the values of P, P_r, and P_t—the polarization parameter, the recoil proton polarization, and the target polarization, respectively. The values of P were taken from Refs. 8 and 9. The determination of P_r was discussed above. P_t was measured by the standard nuclear magnetic resonance techniques. Although our recorded data also permitted a determination of the elastic p-p polarization parameter with high statistical accuracy, we utilized published P values to avoid any biases due to the veto action of the polarimeter computer. Such biases, which can significantly affect the apparent relative flux normalization for the two target enhancements in the measurement of P, have no effect on the measurement of the recoil proton polarization P_r. A PDP-15 on-line computer system recorded data from all particle detectors in the experiment and the parameters of the PPT system and transmitted this information to magnetic tape after each filling of a 46-event buffer. The on-line computer was also used to monitor all critical aspects of the experiment.

The measured values of D are given in Table I and in Fig. 7. In addition to the statistical errors shown, a systematic uncertainty of ~±10% exists due to uncertainties in the analyzing power, the polarization parameter and instrumental asymmetries. Figure 7 also contains the measurement reported in Ref. 10. We note that D is positive at all points measured and that for $|t| < 1$ (GeV/c)^2 D does not deviate drastically from unity. This implies that at small $|t|$ the spin of the target proton is not violently changed by the scattering process. An alternative statement is that the two amplitudes φ_1 and φ_3 are of comparable magnitude over this $|t|$ region (again assuming that the double flip amplitudes φ_2 and φ_4 are negligible). On the other hand we should also note that, if the value of D near $|t| = 0.4$ (GeV/c)^2 is indeed as low as 0.80, then one amplitude could be as much as twice the other amplitude at this t value, in contrast to the usual assumption that they are approximately equal.

The quantity $1 - D$ is determined by the amplitude combinations $\varphi_1 - \varphi_3$ and $\varphi_2 + \varphi_4$, which can be shown to receive contributions in the t channel only from unnatural parity exchanges.[11] Since such exchanges are expected to be negligible for p-p elastic scattering, the exchange-model prediction for D at small $|t|$ is $D \cong 1$. This prediction is not inconsistent with our results. High-precision depolarization measurements at small $|t|$ would be valuable in further testing the applicability of the simple Regge-exchange model to p-p elastic scattering at intermediate momenta. Our depolarization results are also of interest for s-channel models such as the Chu-Hendry[12] optical model; the deviation of $1 - D$ from zero indicates how different the impact-parameter distributions of φ_1 and φ_3 are. The solid line in Fig. 7 illustrates a typical fit with this kind of model[12]; the three amplitudes φ_1, φ_3, and φ_5 are used to fit the differential cross section, polarization, and depolarization simultaneously.

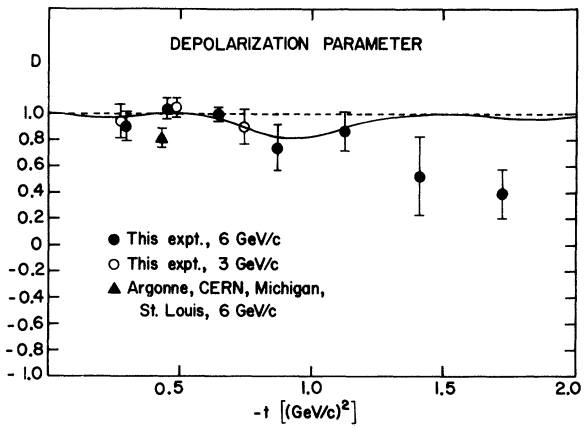

FIG. 7. The depolarization parameter vs t. The solid circles represent data from the present experiment at 6 GeV/c. The open circles represent data from the present experiment at 3 GeV/c. The solid triangle is a measurement at 6 GeV/c reported in Ref. 10. The solid line represents a fit to the data with the parametrization of the Chu-Hendry optical model (Ref. 12).

We wish to express our gratitude to the Argonne ZGS staff for its generous support during the installation and execution of this experiment. We also wish to acknowledge the dedicated services of our group members M. Alam, S. Ems, J. Krider, M. Morrison, and H. Petri.

---

*Work supported by the U. S. Energy Research and Development Administration under Contract No. AT(11-1)-2009, Tasks A and B, and by the Alfred P. Sloan Foundation.

†Present address: Department of Physics, State University of New York at Stony Brook, Stony Brook, N. Y. 11794.

‡Alfred P. Sloan Foundation Fellow.

[1]L. Wolfenstein, Phys. Rev. 96, 1654 (1954).

[2]M. L. Goldberger, M. T. Grisaru, S. W. MacDowell, and D. Y. Wong, Phys. Rev. 120, 2250 (1960).

[3]C. R. Schumacher and H. A. Bethe, Phys. Rev. 121, 1534 (1961).

[4]Two different target materials were utilized in the experiment. For the 3-GeV/c running ethylene glycol was used. For the 6-GeV/c running propanediol was used.

[5]G. W. Abshire, C. M. Ankenbrandt, R. R. Crittenden, R. M. Heinz, K. Hinotani, S. I. Levy, H. A. Neal, and D. R. Rust, Phys. Rev. D 9, 555 (1974).

[6]P. H. Surko, Lawrence Radiation Laboratory Report No. UCRL-19451, 1970 (unpublished).

[7]H. A. Neal and M. J. Longo, Phys. Rev. 161, 1374 (1967); H. A. Neal, Univ. of Mich. Technical Report No. 03106-23-T, 1966 (unpublished).

[8]J. H. Parry, N. E. Booth, G. Conforto, R. J. Esterling, J. Scheid, D. J. Sherden, and A. Yokosawa, Phys. Rev. D 8, 45 (1973).

[9]M. Borghini, L. Dick, L. Di Lella, A. Navarro, J. C. Olivier, K. Reibel, C. Coignet, D. Cronenberger, G. Gregoire, K. Kuroda, A. Michalowicz, M. Poulet, D. Sillou, C. Bellettini, P. L. Braccini, T. Del Prete, L. Foà, G. Sanguinetti, and M. Valdata, Phys. Lett. 31B, 405 (1970).

[10]R. C. Fernow, S. W. Gray, A. D. Krisch, H. E. Miettinen, J. B. Roberts, K. M. Terwilliger, W. DeBoer, E. F. Parker, L. G. Ratner, and J. R. O'Fallon, Phys. Lett. 52B, 243 (1974).

[11]E. Leader and R. C. Slansky, Phys. Rev. 148, 1491 (1966).

[12]S.-Y. Chu and A. W. Hendry, Phys. Rev. D 6, 190 (1972); T. Y. Cheng, S.-Y. Chu, and A. W. Hendry, *ibid.* 7, 86 (1973).